Cell, Vol. 105, 81–91, April 6, 2001, Copyright ©2001 by Cell Press

Drosophila Rho-Associated Kinase (Drok) Links Frizzled-Mediated Planar Cell Polarity Signaling to the Actin Cytoskeleton

Christopher G. Winter,* Bruce Wang,* Anna Ballew,*† Anne Royou,‡ Roger Karess,‡ Jeffrey D. Axelrod,† and Liqun Luo*§

*Department of Biological Sciences
Stanford University
Stanford, California 94305
†Department of Pathology
Stanford University School of Medicine
Stanford, California 94305
‡CNRS
Centre de Génétique Moléculaire
UPR 2167
Avenue de la Terrasse
91198 Gif sur Yvette
France

Summary

Frizzled (Fz) and Dishevelled (Dsh) are components of an evolutionarily conserved signaling pathway that regulates planar cell polarity. How this signaling pathway directs asymmetric cytoskeletal reorganization and polarized cell morphology remains unknown. Here, we show that *Drosophila* Rho-associated kinase (Drok) works downstream of Fz/Dsh to mediate a branch of the planar polarity pathway involved in ommatidial rotation in the eye and in restricting actin bundle formation to a single site in developing wing cells. The primary output of Drok signaling is regulating the phosphorylation of nonmuscle myosin regulatory light chain, and hence the activity of myosin II. *Drosophila* myosin VIIA, the homolog of the human Usher Syndrome 1B gene, also functions in conjunction with this newly defined portion of the Fz/Dsh signaling pathway to regulate the actin cytoskeleton.

Introduction

A fundamental problem in cell and developmental biology is to understand how cytoskeletal architecture is organized in response to extracellular signals, giving rise to tissue and cell-specific morphology. In neurons, guidance cues instruct the polarized growth of axons and dendrites to their synaptic targets. Epithelial cells are polarized along their apical/basal axis and, in many cases, along the orthogonal axis within the plane of the tissue. An example of this planar cell polarity (PCP) is seen within the sensory epithelium of the vertebrate inner ear. The apical surface of each hair cell contains a single sensory transduction unit that is composed of numerous actin-based stereocilia ordered by height, forming a staircase-like arrangement (Tilney and Tilney, 1992). This precisely polarized organization is essential for auditory and vestibular sensory function. Mutations in myosin VIIA, which is highly expressed in the inner ear sensory epithelia (Hasson et al., 1997), lead to inner ear defects and deafness in both mice (*shaker-1* mutant) and humans (Usher syndrome 1B; reviewed in Friedman et al., 1999). Developmental analysis revealed that in the *shaker-1* mutant mouse, the stereocilia on each cell are divided into multiple, disorganized groups (Self et al., 1998), suggesting a possible defect in the establishment of PCP.

PCP has been most extensively studied in the context of eye and wing development in *Drosophila* (reviewed in Shulman et al., 1998; Mlodzik, 1999). During the development of the compound eye, trapezoid-shaped clusters of photoreceptors adopt a specified chirality and orientation. Mutations in genes that regulate PCP result in failure of ommatidia to acquire the correct chirality, and/or failure to rotate properly. In the wing, PCP is evident in the uniform pattern formed by distally oriented hairs that cover the dorsal and ventral surfaces. Each cell constructs a single wing hair derived from a prehair composed largely of bundled actin filaments assembled at the distal vertex of the hexagon-shaped cells during pupal development (Wong and Adler, 1993). Mutants in PCP signaling have characteristic defects in both the orientation and number of wing hairs per cell (Gubb and Garcia-Bellido, 1982; Wong and Adler, 1993).

Genetic analyses have led to a model for PCP signaling in which cells receive and interpret information from the extracellular environment and translate these signals into changes in both cytoskeletal polarity and transcription (Shulman et al., 1998; Mlodzik, 1999). The seven-pass transmembrane protein, Frizzled (Fz) (Vinson et al., 1989), likely acts as a receptor, and requires the downstream signaling protein Dishevelled (Dsh) (Klingensmith et al., 1994; Theisen et al., 1994; Krasnow et al., 1995). Dsh and Fz family proteins also participate in the Wingless (Wg)/Wnt signal transduction system that regulates a wide variety of developmental events, including cell proliferation and cell fate specification (reviewed in Wodarz and Nusse, 1998). However, Wg and PCP signaling appear to use distinct pathways downstream of Dsh (Axelrod et al., 1998; Boutros et al., 1998). PCP signaling proceeds through several unique components including Flamingo, a novel cadherin (Usui et al., 1999), and the small GTPase RhoA/Rho1 (Strutt et al., 1997). Studies of dominant-negative and active forms of Rac1 suggest that it may also function in PCP signaling (Eaton et al., 1996; Fanto et al., 2000). In addition, a number of tissue-specific factors may participate in interpreting the Fz/Dsh signal (Shulman et al., 1998; Mlodzik, 1999). This morphogenetic pathway appears to be evolutionarily conserved, as it has been shown to regulate convergent extension during vertebrate embryonic development (reviewed in Sokol, 2000).

Ultimately, the PCP signal from Fz/Dsh is expressed as asymmetric cytoskeletal structure. Identification of the small GTPase RhoA as a downstream component of the Fz/Dsh pathway offered some clues as to how this signaling pathway could relay its information to the cytoskeleton. RhoA acts as a molecular switch that

§To whom correspondence should be addressed (e-mail: lluo@stanford.edu).

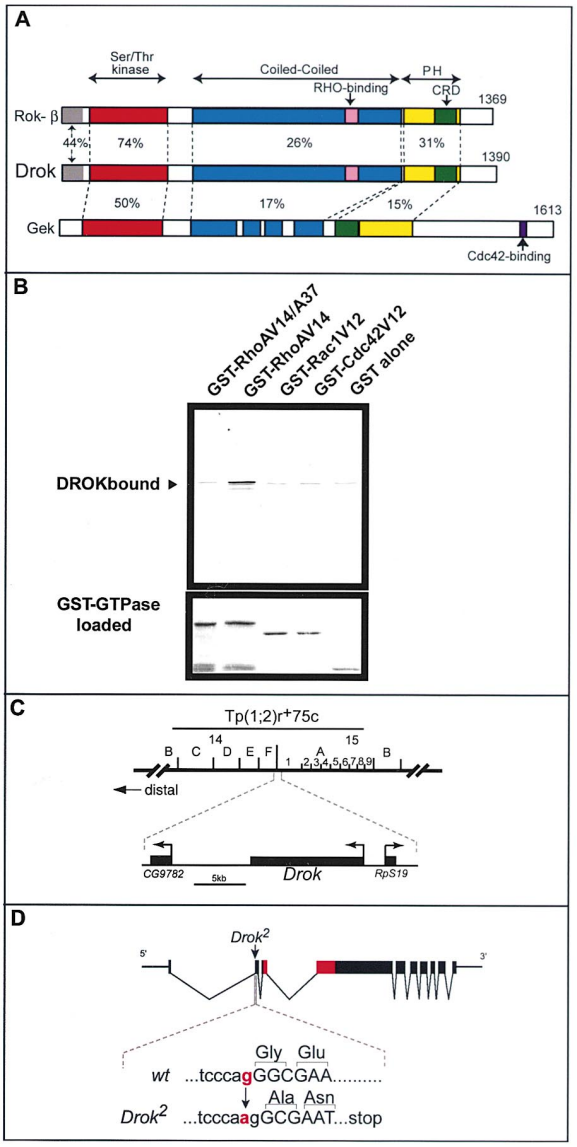

Figure 1. Characterization of Drok Protein and Generation of Loss-of-Function Mutants

(A) Domain structure of Drok compared to rat Rok-β and *Drosophila* Gek. The N-terminal (gray) and other domains are color coded. The most similar *Drosophila* protein to Drok is Gek. Percent amino acid identities are given for each domain.

(B) Drok/GTPase binding assays. The lower panel shows protein levels of various GST fusions revealed by Coomassie staining of the same gel.

(C) Genomic map of *Drok* region.

(D) Molecular identity of the $Drok^2$ mutation. The consensus guanine at the splice acceptor site between intron1 and exon2 is mutated to adenine (highlighted in red).

gates signaling to downstream targets, both nuclear and cytoskeletal, by cycling between its active GTP-bound form and inactive GDP-bound form (Hall, 1998). During eye development, RhoA signals via Jun N-terminal kinase (JNK) and Jun to regulate Fz/PCP-dependent transcription (Strutt et al., 1997; Weber et al., 2000; Fanto et al., 2000). However, it has remained unclear how the Fz/Dsh pathway regulates the formation of polarized cytoskeletal structure.

We report here that a RhoA effector protein, the *Drosophila* Rho-associated kinase (Drok), functions to regulate the actin cytoskeleton downstream of Fz/Dsh. Drok controls a subset of the PCP response: regulating the number but not the orientation of wing hairs, and the rotation but not chirality of photoreceptor clusters. We show that the major signaling output from Drok is the phosphorylation of nonmuscle myosin II regulatory light chain (MRLC) and regulation of myosin II activity. Finally, we show that fly myosin VIIA, homolog of the human Usher Syndrome 1B and mouse *shaker-1* genes, also displays strong genetic interactions with this newly defined Fz/Dsh cytoskeletal signaling pathway. These data provide the first link between Fz/Dsh signaling and direct modulators of the cytoskeleton, and suggest that such a pathway is evolutionarily conserved during the development of epithelial polarity.

Results

Drok as a Downstream Effector of *Drosophila* RhoA

We have reported a multidomain protein kinase, Gek, that binds specifically to the GTP-bound form of *Drosophila* Cdc42 and may serve as an effector for Cdc42 (Luo et al., 1997). We hypothesized that there might be additional Gek-like kinases that serve as effectors for other Rho-family GTPases. Using degenerate PCR, we identified the *Drosophila* homolog of a class of mammalian Rho-associated kinases/ROCKs (Ishizaki et al., 1996; Leung et al., 1996; Matsui et al., 1996), which we named Drok for *Drosophila* Rho-associated kinase. In the course of our studies, Mizuno et al. (1999) have independently reported the identification of Drok. Figure 1A depicts the domain organization of Drok in comparison with rat ROK-β. Both proteins are composed of a conserved N-terminal domain, a serine/threonine kinase domain, a large coiled-coil domain with an embedded Rho-binding domain, and a C-terminal Plekstrin-homology (PH) domain split by a Cys-rich domain (CRD).

To test the physical interaction between Drok and various Rho-GTPases, we employed a pull-down assay using GST-GTPase fusion proteins and in vitro translated Drok. Drok bound to the constitutively active form of *Drosophila* RhoA (Figure 1B, lane 2), but not to constitutively active Rac1 or Cdc42 (lanes 3–4). Mutating a key amino acid within the effector-binding domain (T37A) abolished the interaction with Drok (lane 1). These results, together with those from Mizuno et al. (1999), suggest that Drok is an effector specific for *Drosophila* RhoA.

Generation of *Drok* Mutants

The *Drok* gene was mapped to chromosome region 15A1 on the X chromosome (Figure 1C). To generate loss-of-function mutations in *Drok*, we made the assumption that hemizygous *Drok* mutant males would be lethal, but that such lethality could be rescued by either a genomic duplication that covers the region [*Tp(1;2)r*$^+$*75c*] or by a *Drok* cDNA expressed under the control

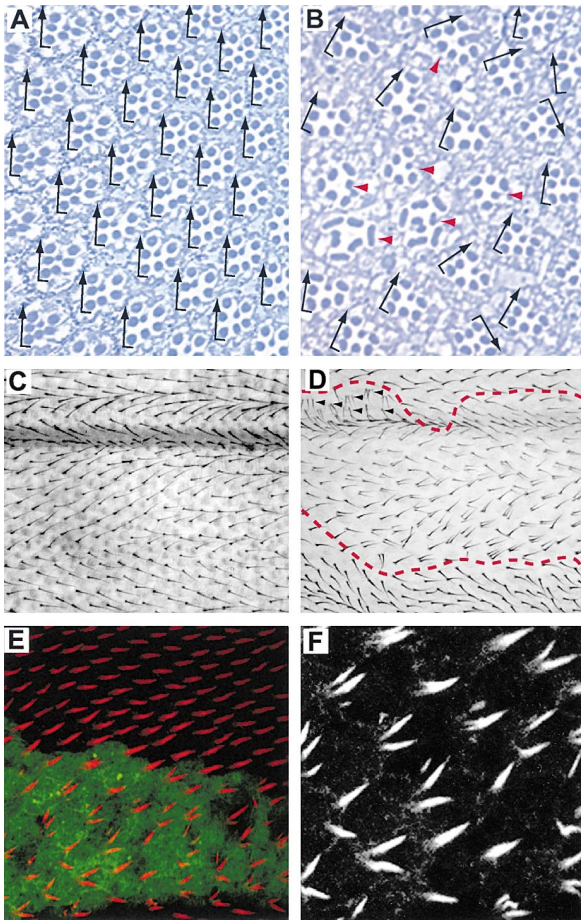

Figure 2. Defects in Epithelial Polarity Resulting from Loss of *Drok* Function

(A and B) Tangential sections of somatic clones in the adult eye showing the arrangement of photoreceptors and orientation of the ommatidia (denoted by arrows) in the ventral half of the eye (ventral is down and anterior to the left) in control (A) and *Drok*^{2} (B) clones.
(C and D) Trichomes on the adult wing in wild type (C) and a *Drok*^{2} mosaic (D). The clonal border is marked with a red dotted line. Arrowheads indicate the rare misorientation of hairs from *Drok*^{2} cells near the wing vein. Some distortion of wing hair orientation occurred during mounting due to the fragile nature of the wing hairs in newly eclosed adult (that allowed the visualization of GFP for marking the clone).
(E) *Drok*^{2} mosaic pupal wing. Homozygous tissues are marked in green with mCD8GFP. Phalloidin (red) staining reveals the multiple F-actin prehairs from *Drok*^{2} mutant cells.
(F) A magnified image of the F-actin structure in *Drok*^{2} mutant cells.
Genotypes: Clone in (A) and whole tissue in (C) are homozygous for *y,w,FRT*^{19A}; clones in (B), (D), (E), and (F) are homozygous *for y,w, Drok*^{2}, *FRT*^{19A}.

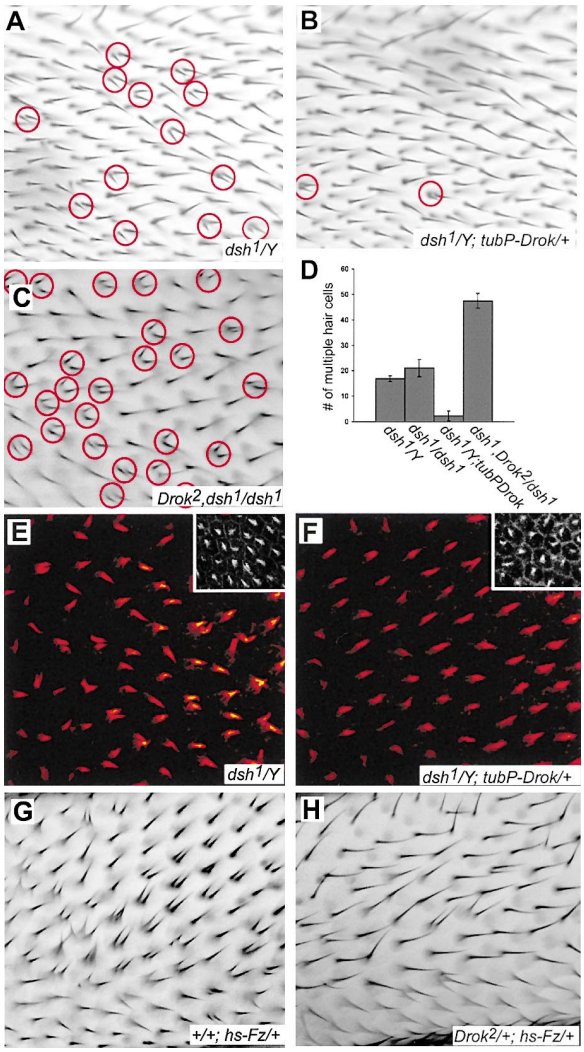

Figure 3. Evidence that Fz/Dsh Function through Drok in Restricting Wing Hair Number

(A–D) Representative multiple hair phenotypes (circled in red) of various genotypes (A–C) in a defined region of the adult wing. Quantified in (D).
(E and F) F-actin staining of pupal *dsh*^{1} wings. Overexpression of Drok (F) suppresses the assembly of ectopic F-actin-rich prehairs in *dsh*^{1} wings cells, but does not suppress the abnormal assembly of the prehair at the center of the cell (insets).
(G and H) The adult wing hair phenotype resulting from elevated Fz activity. Quantified in Table 1.

of the ubiquitously active tubulin-1α promoter (*tubP-Drok*). Screening EMS mutagenized flies led to the identification of two X-linked lethal mutants that were rescued by *Tp(1; 2)r*$^+$*75c* and *tubP-Drok*, and failed to complement each other. These were named *Drok*^{1} *and Drok*^{2}.

To determine the molecular nature of the *Drok* mutations, we performed genomic sequencing of the mutant DNA. The coding sequence of *Drok* is composed of 10 exons (Figure 1D). A single nucleotide transition of G to A was found in the *Drok*^{2} mutant at the 3′ end of intron 1, changing the conserved AG at the splice acceptor site to AA. Quantitative RT-PCR revealed no change in the transcript level in *Drok*^{2} hemizygous larvae compared to control (not shown). However, sequence analysis of the *Drok*^{2} mutant cDNA revealed that the transcript has a single base deletion of guanine at the beginning of exon 2, due to the use of a splice acceptor site one nucleotide 3′ of the original site (Figure 1D). The mutant mRNA encodes only the first 21 amino acids (aa) of Drok, followed by a 35 aa random peptide and a stop

Table 1. Genetic Interactions with *Frizzled* Gain-of-Function Phenotype

Genotype	Interaction*	Multiple wing hair cells/sector		
		Avg.	Std. Error	N
hs-Fz/+; +/+	—	71.1	(±4.0)	15
hs-Fz/+; wg^{1g22}/+	no effect	71.7	(±3.9)	15
hs-Fz/+; dsh^{1}/+	suppression	21.1	(±2.8)	8
hs-Fz/+; $Drok^{2}$/+	suppression	29.4	(±3.6)	11
hs-Fz/+; sqh^{AX3}/+	suppression	31.5	(±5.3)	12
hs-Fz/+; $RhoA^{72O}$/+	suppression	34.1	(±3.4)	10
hs-Fz/+; zip^{1}/+	enhancement	94.3	(±4.0)	10
hs-Fz/+; ck^{13}/+	suppression	7.6	(±1.4)	10

Genetic interactions were scored as the effect of loss of one wild-type copy of the genes tested on the expressivity of the multiple wing hair phenotype resulting from heat shock–induced overexpression of Fz at 30 h APF.
*Interaction: statistical significance was determined by Student's t-test ($p < 0.001$).

codon, before the start of the kinase domain (red). Hence, $Drok^{2}$ is likely to be a strong loss-of-function, if not a null mutation. Since we have not yet identified the molecular nature of the $Drok^{1}$ mutation, we used the $Drok^{2}$ allele for the rest of this study.

Drok Is Essential for a Specific Subset of Epithelial Polarization Events

The *Drok* transcript is ubiquitous in all stages of embryogenesis and in imaginal discs (not shown; Mizuno et al., 1999). $Drok^{2}$ mutants die before developing into wandering 3rd instar larvae. To investigate the function of *Drok* in the morphogenesis of adult tissues, we examined somatic $Drok^{2}$ clones generated by mitotic recombination.

Homozygous $Drok^{2}$ clones in the eye are of similar size as their wild-type siblings (twin spots), indicating no gross defects in proliferation or survival of $Drok^{2}$ mutant cells. However, about 50% of ommatidia exhibited increase or decrease in photoreceptor numbers (Figure 2B, arrowheads). A change of photoreceptor number has also been reported in eye clones homozygous for a hypomorphic *RhoA* allele (Strutt et al., 1997). Of those ommatidia with the correct number of photoreceptors, 60% were misrotated (Figure 2B), whereas in control clones all ommatidia were properly rotated (Figure 2A). These phenotypes resemble those of PCP mutants such as *fz*, *dsh*, and *RhoA* (reviewed in Mlodzik, 1999), suggesting that *Drok* may also participate in the signaling cascade controlling PCP. Unlike *fz* and *dsh*, however, very few ommatidia showed aberrant chirality.

We also examined the function of *Drok* in the wing, where PCP is exhibited at a single cell level (Wong and Adler, 1993). In wild-type wings, each cell produces a single, distally oriented wing hair (Figure 2C), while in $Drok^{2}$ adult wing clones, greater than 70% of the cells produce multiple hairs (Figure 2D). In contrast to most known PCP genes, including *fz* and *dsh*, which exhibit both stereotypical orientation and multiple hair defects (Gubb and Garcia-Bellido, 1982; Wong and Adler, 1993), most hairs within $Drok^{2}$ clones maintain a largely distal orientation (Figure 2D).

To investigate the nature of the *Drok* phenotype during the development of wing cell polarity, we used phalloidin to examine the F-actin distribution in $Drok^{2}$ clones during prehair initiation (Figure 2E, red). Mutant clones were positively marked using the MARCM strategy (Lee and Luo, 1999) (Figure 2E, green). In control clones (not shown) or in heterozygous tissue neighboring $Drok^{2}$ mutant clones (Figure 2E), each wing cell generates a single F-actin bundle from its distal vertex, extending toward its distal neighbor. However, in $Drok^{2}$ clones, a majority of the cells generate more than one F-actin bundle. The F-actin-based prehairs always initiate at the cell periphery (Figure 2F). Notably, the majority of the prehairs maintain a roughly distal orientation (in the case of multiple hairs, the vector average remains distal). The similarities between the pupal and adult clonal phenotypes indicate that the multiple hair phenotype of adult $Drok^{2}$ clones is likely the result of failure to restrict F-actin bundle assembly to a single site during prehair formation.

The multiple hair/actin phenotype was seen only in mutant cells and never in neighboring heterozygous or wild-type cells (Figures 2D and 2E), indicating that *Drok* acts in a cell-autonomous manner.

Evidence that *Drok* Acts Downstream of *fz*/*dsh*

The similarity of the $Drok^{2}$ clonal phenotype in the wing to aspects of the phenotypes of *fz*, *dsh*, and *RhoA* led us to hypothesize that Drok may act downstream of Fz/Dsh. To assess the genetic interactions among these genes, we quantified the multiple hair phenotype in a defined region, the ventral surface of the proximal-anterior region of the wing.

We made use of the dsh^{1} allele, which is defective for PCP function without affecting Wg signaling (Axelrod et al., 1998; Boutros et al., 1998). In dsh^{1} hemizygous males, an average of 16.8 cells with multiple hairs (12% of the cells) are present in this region (Figure 3A). When Drok was overexpressed via a *tubP-Drok* transgene in the dsh^{1} hemizygous background, the average number of cells exhibiting multiple hairs was reduced by more than 7-fold to 2.3 per wing region (Figures 3B and 3D). *tubP-Drok* expression in a wild-type genetic background did not give rise to any obvious phenotypes (data not shown). Suppression of the dsh^{1} multiple hair phenotype by *tubP-Drok* expression could also be seen when F-actin-based prehairs were visualized in the pupal wing (Figures 3E and 3F). In contrast to the suppression of the dsh^{1} phenotype by overexpression of Drok, reduction of *Drok* dosage by 50% (assuming that $Drok^{2}$

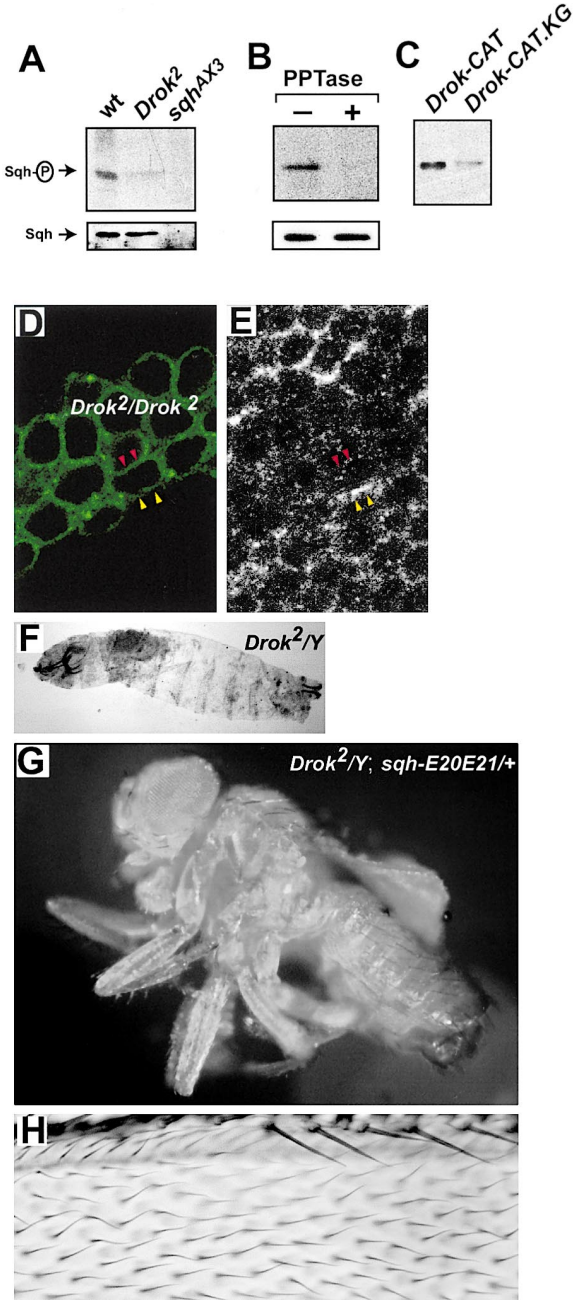

Figure 4. Regulation of Sqh Phosphorylation by Drok In Vivo

Upper panels: Immunoblots of phosphorylated Sqh detected with anti-phospho-MRLC antibody. Lower panels: Duplicate blots probed with anti-Sqh antibody.

(A) 1st instar larval extracts of wild type, *Drok*^{2}/Y, *sqh*^{AX3}/Y.

(B) Untreated (−) and phosphatase-treated (+) wild-type extracts.

(C) *hs-GAL4>UAS-Drok-CAT (Drok-CAT)*, and *hs-GAL4>UAS-Drok-CAT.KG(Drok-CAT.KG)*.

(D and E) Confocal images of the same wing cells at 32 hr APF visualized by GFP (D) or anti-phospho-MRLC (E). Homozygous *Drok*^{2} wing cells are marked with green in (D). Red arrowheads: cell membranes between two *Drok*^{2}/*Drok*^{2} cells; yellow arrowheads: cell membranes between a *Drok*^{2}/ *Drok*^{2} cell and a *Drok*^{2}/+ (or +/+) cell.

(F) A dead second instar *Drok*^{2} mutant larva, representative of the lethal phase of the mutant population.

(G) A *Drok*^{2} mutant fly rescued from larval lethality to viable adult by the presence of a single copy of a *sqhE20E21* transgene.

(H) The wing of a *sqhE20E21* rescued *Drok*^{2}/Y adult fly lacks multiple hair.

is null) resulted in a 2.5-fold increase in the number of multiple hair cells (Figures 3C and 3D).

We also examined genetic interactions between *Drok* and *fz* in a different assay. The proper level of Fz/Dsh signaling is critical for the generation of wild-type PCP, as both overexpression and loss of function of these genes result in polarity defects in the eye (Zheng et al., 1995; Strutt et al., 1997) and the wing (Krasnow and Adler, 1994). Overexpression of Fz 30 hr after puparium formation (APF) produced primarily a multiple hair phenotype that was suppressed by *dsh*^{1} heterozygosity (Table 1; Krasnow and Adler, 1994). Similarly, reducing the wild-type copy number of *RhoA* and *Drok* by half suppressed the phenotype by 2- to 2.5-fold (Figures 3G and 3H; Table 1). Taken together, these experiments suggest that Drok functions downstream of Fz/Dsh in restricting the number of F-actin-based prehairs.

Nonmuscle Myosin II Regulatory Light Chain: A Critical Drok Target

Studies in mammalian cells have identified several downstream substrates for Rho-kinase/ROCK (Amano et al., 2000). In particular, Rho-kinase regulates the phosphorylation of the nonmuscle myosin regulatory light chain (MRLC) primarily at Ser-19 and secondarily at the adjacent Thr-18 (Amano et al., 1996; Kimura et al., 1996). Phosphorylation of MRLC at these sites results in a conformational change that allows myosin II to form filaments and increases its actin-dependent ATPase activity (reviewed in Tan et al., 1992).

The amino acid sequence around the phosphorylation site of MRLC is highly conserved between mammalian MRLC and the *Drosophila* homolog, encoded by *spaghetti squash* (*sqh*) (Karess et al., 1991; Jordan and Karess, 1997). We therefore assessed the phosphorylation of the *Drosophila* MRLC using an antibody that recognizes mammalian MRLC only when Ser-19 is phosphorylated (anti-phosho-MRLC; Matsumura et al., 1998). Immunoblot analysis showed that this antibody specifically recognizes phosphorylated Sqh in larval extracts (Figure 4A)—the single ~20 kDa band in wild-type extract is absent in extracts of a *sqh* null, or when wild-type extract is treated with phosphatase (Figure 4B). While phosphorylated Sqh is detectable in *Drok*^{2} mutant extracts, its level is greatly reduced (Figure 4A), whereas the Sqh protein level is not affected in *Drok*^{2} mutants (Figure 4A, lower panel). Previous work with bovine Rho-kinase established that expression of the N-terminal catalytic domain gives rise to a constitutively active kinase (Amano et al., 1997). Raising the level of Drok activity in vivo by transient expression of the catalytic domain of Drok (Drok-CAT) resulted in elevated phosphorylation of Sqh as compared to controls in which a kinase-dead form (Drok-CAT-KG) was expressed (Figure 4C). Taken together, these experiments indicate that Drok is required for maintaining the proper level of MRLC phosphorylation in vivo, and that such regulation depends on its kinase activity.

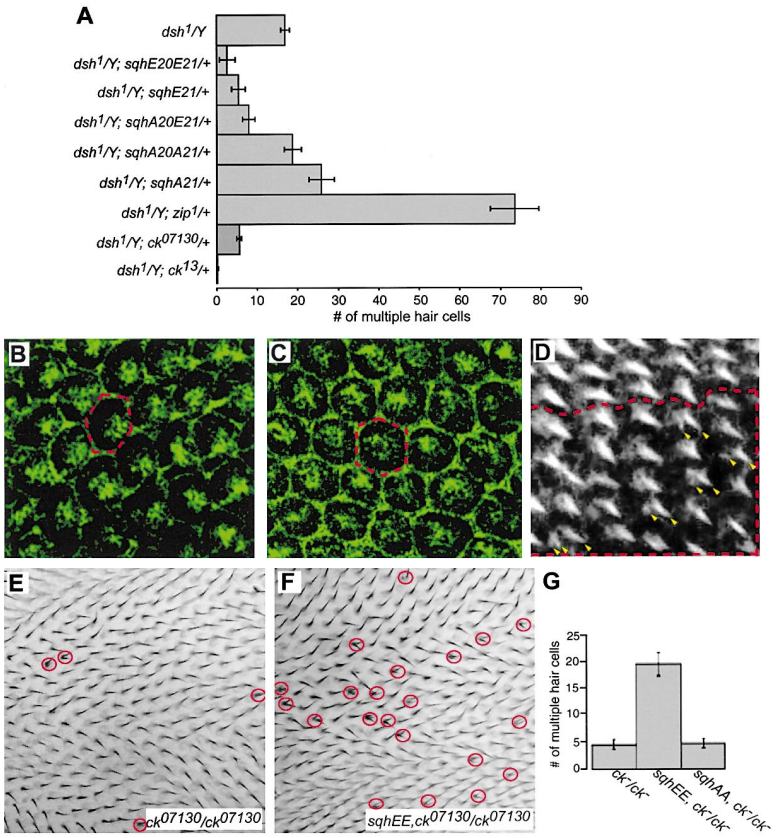

Figure 5. The Role of Myosin II (*sqh* and *zip*) and Myosin VIIA (*ck*) in the Regulation of Wing Hair Number

(A) Quantification of multiple hair phenotypes modified by *sqh* transgenes with single or double amino acid substitutions at Thr-20 and Ser-21, or by heterozygosity of the zip^{1} (null), ck^{13} (strong), or ck^{07130} (weak) mutations (FlyBase).

(B–C) Confocal images of Zip immunoreactivity in the pupal wing. Red dots outline the plasma membrane of a single cell.

(D) Phalloidin staining of a clone (within red dotted area) homozygous for a hypomorphic zip^{02957} allele. Multiple F-actin prehairs are indicated by yellow arrowheads.

(E and F) Multiple hair (red circle) phenotypes in ck^{07130} variants (genotypes indicated).

(G) Quantification of the effect of expressing *sqhE20E21* and *sqhA20A21* on the ck^{07130} homozygous phenotype.

Error bars in (A) and (G) represent standard errors.

We also examined the effect of loss of Drok function on MRLC phosphorylation at the cellular level. In wild-type wing cells, phosho-MRLC is enriched at the cortex of the pupal wing cells, whereas in $Drok^{2}$ mutant cells this perimembrane staining is reduced or absent (Figures 4D and 4E). Thus, *Drok* is cell autonomously required for maintaining the level of cortical phospho-MRLC in the pupal wing.

Next, we tested whether MRLC/Sqh is an effector for Drok in regulating hair number in response to Fz/Dsh signaling. We made use of a series of mutant *sqh* transgenes with point mutations in the primary (Ser-21) and secondary (Thr-20) phosphorylation sites, changing them either to glutamic acid (phosphomimetic), or to nonphosphorylatable alanine. These *sqh* transgenes are under control of the endogenous promoter and are expressed at levels similar to the native protein (Jordan and Karess, 1997). Remarkably, whereas 100% of $Drok^{2}$ hemizygous animals die before the wandering third instar stage, introducing one copy of a *sqh* transgene carrying the E20E21 double mutation (mimicking phosphorylation on both sites) resulted in 4% hemizygous $Drok^{2}$ survival to adulthood (Figures 4F and 4G). Likewise, one copy of an analogous transgene expressing SqhE21 also resulted in $Drok^{2}$ hemizygotes surviving to adulthood (albeit a lower percentage), with a large fraction surviving to late-stage pupae. No rescue was observed when transgenes expressing the alanine substituted forms (SqhA20A21 or SqhA21) were introduced into the $Drok^{2}$ background. These observations support the notion that MRLC is a key target (either directly or indirectly) for Drok kinase in vivo, since mimicking its phosphorylation, even in an unregulated fashion, partially rescues $Drok^{2}$ organismal lethality.

Moreover, the multiple hair defect resulting from *Drok* loss of function is almost completely suppressed by the presence of the *sqhE20E21* transgene in the rescued adults (Figure 4H; from 70% without *sqhE20E21* to $<1\%$ in its presence). Taken together with the modulation of MRLC phosphorylation by Drok (Figures 4A–4C), these results demonstrate that the regulation of MRLC phosphorylation is a principal function of Drok in regulating F-actin prehair number.

Nonmuscle Myosin II in Fz/Dsh Signaling

To test whether the phosphorylation state of MRLC can also modulate Fz/Dsh signaling, we assayed whether the phosphomimetic and nonphosphorylatable forms of MRLC can directly modify the dsh^{1} multiple hair phenotype. Introducing one copy of *sqhE20E21* reduced the number of multiple hair cells in dsh^{1} mutants by 5-fold (Figure 5A). *sqhE21*, or *sqhA20E21*, also suppressed the dsh^{1} phenotype by more than 2-fold. In contrast, introduction of *sqhA21* into the dsh^{1} background enhanced the multiple hair phenotype. We also tested the involvement of MRLC in the Fz/Dsh pathway using the Fz-overexpression assay. Reducing the wild-type *sqh* gene dosage from two to one, by introducing a single copy of the sqh^{AX3} null allele (Jordan and Karess, 1997), resulted in a 2-fold suppression of the multiple hair phenotype caused by Fz overexpression (Table 1). These results support the notion that MRLC functions in the

PCP pathway to restrict F-actin bundle assembly to a single site.

MRLC phosphorylation in response to Drok activation would be predicted to modify the conformation and elevate the catalytic activity of its associated heavy chain, Zipper (Zip) (Young et al., 1993). We tested whether Zip also participates in regulating actin distribution/wing hair number in response to Fz/Dsh. Loss of one copy of the *zip* gene enhanced the *dsh*^{1} phenotype by 4.5-fold (Figure 5A), consistent with the genetic interaction data between *fz*/*dsh* and *sqh*. These results suggest that myosin II functions positively downstream of Fz/Dsh in regulating actin prehair development.

The localization of Zip protein in wing cells further supports its role downstream of Fz/Dsh. At the apical surface of the pupal wing cell, Zip is asymmetrically localized to the distal portion of the cell, where prehair growth initiates (Figure 5B). This distal localization appears to coincide, temporally, with prehair initiation. To test whether Zip localization could be modified by Fz/Dsh signaling, we examined Zip distribution at the apical surface in *dsh*^{1} mutants. Instead of being concentrated in the distal region of the cell, Zip was concentrated in the center of the cell (Figure 5C), where prehairs form in *dsh*^{1} mutants (Wong and Adler, 1993).

Finally, we tested whether reduction in myosin II/Zip activity also results in the multihair phenotype. We made use of the hypomorphic *zip*^{02957} (Spradling et al., 1999), as *zip* and *sqh* null mutations appear to be cell lethal in the wing (our unpublished observations). As is the case with *Drok*, some homozygous *zip*^{02957} wing cells possess multiple F-actin prehairs (Figure 5D).

MyosinVIIA/*crinkled* also Interacts with Fz/Dsh Polarity Signaling

We also tested if the gene *crinkled* (*ck*) is involved in the Fz/Dsh signaling pathway regulating wing hair number because (1) *ck* mutant cells in the wing lead to multiple hair and split hair phenotypes (Gubb et al., 1984; Turner and Adler, 1998), and (2) *ck* encodes the *Drosophila* myosin VIIA protein (Chen et al., 1991; Ashburner et al., 1999). Mutations in mouse myosinVIIA lead to stereocilia disorganization and the formation of multiple bundles of stereocilia (see Eaton, 1997; Self et al., 1998).

Reduction of *ck* activity potently suppressed the *dsh*^{1} multiple hair phenotype (Figure 5A). This result contrasts with the result that *zip*^{1} enhances the *dsh*^{1} multiple hair phenotype, and suggests that the two myosin heavy chains have opposing effects in regulating prehair assembly.

We then tested both myosin heavy chain genes for their ability to interact with the *hs-fz* induced multiple hair phenotype, and again found that they have opposing effects. Surprisingly, loss of one copy of *zip* slightly but significantly enhanced the late *hs-fz* multiple hair phenotype, while loss of one copy of *ck* markedly suppressed this phenotype (Table 1). These results are the reverse of what one would expect based on their interactions with *dsh*^{1}, and suggests the possibility that there is a signal from Fz to Ck that is independent of Dsh, or that the multiple hair phenotypes resulting from hypo- or hyperactivity of the Fz/Dsh pathway arise via distinct biochemical mechanisms.

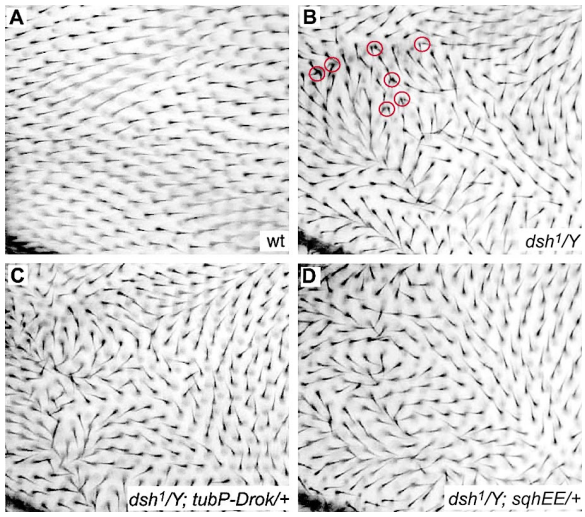

Figure 6. Expression of *tubP-Drok* or *sqhE20E21* Transgenes Does Not Rescue the Orientation Defect in *dsh*^{1} Mutants

Adult wings of wild-type (A), *dsh*^{1} mutant (B) or *dsh*^{1} in the presence of one copy of either a *tubP-Drok* (C) or a *sqhE20E21* transgene (D). The images are of the same region in the 2nd posterior "cell". Multiple hair cells are circled.

To further assess the nature of the relationship between the two myosins, we tested the effect of raising or lowering the activity of MRLC on the *ck* phenotype. The multiple hair phenotype in animals homozygous for a weak *ck* mutation was enhanced by one copy of the *sqhE20E21* transgene (and hence, a probable increase in myosin II activity), but not by a *sqhA20A21* transgene (Figures 5E–5G). Taken together, these experiments suggest that a balance between the activities of myosin II and myosin VIIA is important in regulating wing hair number.

Separate Pathways Regulating Wing Hair Orientation and Number Downstream of Fz/Dsh

Unlike other characterized PCP mutants which affect both orientation and number of wing hairs (Wong and Adler, 1993), the primary defect in *Drok*^{2} clones appears to be the presence of multiple hairs per cell, with little or no wing hair orientation defect. This suggested that Drok and what lies downstream are involved in transmitting a subset of the Fz/Dsh signal. Supporting this idea, we found that *tubP-Drok* and *sqhE20E21* suppressed the multiple hair phenotype of *dsh*^{1}, but not the hair mis-orientation phenotype (Figure 6). Additional data supporting this conclusion came from observing the site of prehair initiation. As previously reported (Wong and Adler, 1993), prehairs emerge aberrantly from the center of *dsh*^{1} mutant cells (Figure 3E, inset), rather than from the distal vertex as seen in wild type cells. Such mispositioning of prehair initiation correlates with the failure to acquire the proper distal orientation (Wong and Adler, 1993). While *tubP-Drok* expression suppressed multiple prehair formation, it did not affect the site of F-actin initiation in *dsh*^{1} (Figure 3F, inset). Finally, the hair orientation defect resulting from Fz overexpression (via *hs-fz*) at 24 hours is suppressed by reducing *dsh* gene dosage

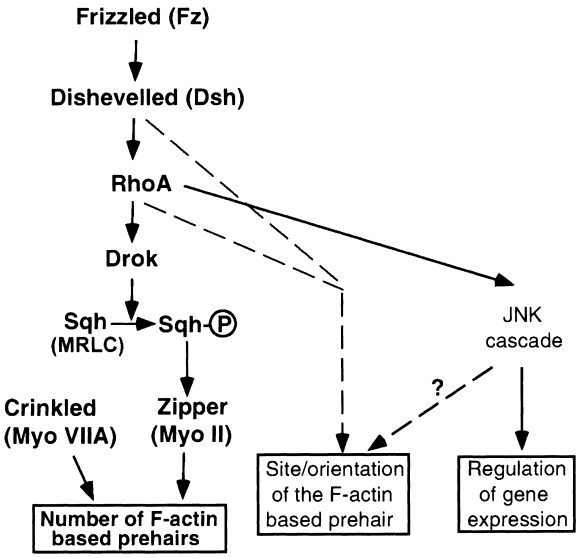

Figure 7. A Model of the Fz/Dsh Polarity Signaling Pathways

Components in bold leading to the regulation of the number of F-actin-based prehairs are subjects of this study. The JNK cascade was established previously (Strutt et al., 1997). Our study also implies a separate pathway downstream of Dsh or RhoA to the cytoskeleton (dashed arrows) that determines the site/orientation of the F-actin-based prehairs.

but not that of *RhoA*, *Drok*, *sqh* or *ck* (data not shown). Taken together, these observations suggest that separate mechanisms allow Fz/Dsh to independently regulate the number and the orientation of prehairs, and that only the former involves Drok signaling.

Discussion

Drok Links Fz/Dsh Signaling to the Actin Cytoskeleton

Mammalian and *C. elegans* Rho-kinase/ROCK have been implicated in regulating actin stress fibers formation in fibroblasts (Leung et al., 1996; Amano et al., 1997; Ishizaki et al., 1997) or changes in hypodermal cell shape during embryonic development (Wissmann et al., 1997). How Rho-kinase/ROCK is regulated by an extracellular signal in a physiological process is unknown. We present several lines of evidence that *Drosophila* Rho-associated kinase is required for restricting the number of sites of F-actin bundle assembly in response to activation of the Fz/Dsh pathway. Together with the previously established genetic link between Fz/Dsh and RhoA (Strutt et al., 1997), a molecular pathway from Fz/Dsh to the regulation of actin structure has been established (Figure 7). Proteins that physically mediate the interaction between Fz and Dsh, and between Dsh and RhoA, remain to be identified.

The data presented here suggest that the Drok/myosin II pathway is involved in regulating the number—but not orientation—of the wing hair. What then are the components that regulate wing hair orientation? One possibility is that a bifurcation of the pathway occurs at the level of RhoA, with a separate effector pathway regulating wing hair orientation. In the eye, the JNK pathway has been implicated in functioning downstream of RhoA in regulating ommatidial polarity (Strutt et al., 1997). However, the function of the JNK pathway in the wing has not been described, and a signaling pathway that regulates transcription is unlikely to encode the requisite spatial information necessary for selection of the site of prehair initiation. Therefore, it is likely that a separate signal from or upstream of RhoA may control the selection of the F-actin assembly site, and therefore the orientation of the wing hair (Figure 7).

Several other genes have been implicated in regulating wing hair number based on their loss-of-function phenotypes, including *inturned (in)*, *fuzzy(fy)*, and *multiple wing hair (mwh)* (reviewed in Shulman et al., 1998). We believe that these gene products participate in a distinct branch of the polarity signaling pathway for the following reasons. First, because they each have significant effects on both hair orientation and hair number, they are unlikely to function downstream of Drok. Second, expression of the phosphomimetic Sqh-E20E21, or the nonactivatable Sqh-A20A21, in *mwh* or *in* mutant backgrounds did not modify their phenotypes (data not shown). Third, while Drok functions in the eye as well as in the wing, In, Fy, and Mwh have no apparent role in PCP signaling in the eye.

The misorientation of ommatidia in $Drok^2$ eye clones is also consistent with its functioning in the Fz/Dsh/RhoA pathway (Strutt et al., 1997). It is conceivable that Drok may act as an effector of RhoA in regulating the process of ommatidial rotation. Alternatively, loss of Drok function could lead to a disruption of the actin cytoskeleton and a consequent loss of the appropriate cell–cell contacts that support intercellular signaling essential for ommatidial rotation (Mlodzik, 1999). Although *Drok* mutants exhibit misrotation of ommatidia, they acquire the proper chiral form. Determination of ommatidial rotation may reflect a Drok-dependent subset of PCP signaling in the eye that is, in some way, molecularly analogous to the subset of PCP signaling in the wing reflected in the regulation of hair number.

Phosphorylation of MRLC as a Major Output of Drok Signaling In Vivo

Biochemical and cell culture studies have identified many potential substrates for Rho-kinase/ROCK (reviewed in Amano et al., 2000) The relative contribution of phosphorylation of these different substrates in mediating various functions of Rho-kinase/ROCK is unclear. We provide strong genetic evidence that phosphorylation of MRLC at key residues (Ser-21 in *Drosophila*, equivalent to Ser-19 in mammals) is a critical output for Drok signaling (Figure 7). Phosphomimetic MRLC expression not only suppressed the multiple wing hair phenotype, but also lethality, of $Drok^2$ mutants. Biochemical and immunostaining experiments further demonstrate that Drok modulates MRLC phosphorylation in vivo. Previous work has suggested that Drok regulates phosphorylation of MRLC both by direct phosphorylation and also by phosphorylation and inhibition of the myosin binding subunit of myosin phosphatase (MBS) (Amano et al., 2000). However, we do not know at present the relative contribution of direct phosphorylation by Drok of MRLC, versus phosphorylation of MBS that indirectly affects MRLC phosphorylation.

The direct genetic interactions between *dsh*^{1} and various *sqh* transgenes further substantiate the notion that regulation of MRLC phosphorylation is not only a major output of Drok signaling, but also of Fz/Dsh signaling to the actin cytoskeleton in regulating hair number.

Possible Mechanisms of Myosin II in Regulating F-Actin Bundle Assembly

By what mechanism do myosins restrict F-actin bundle formation? In light of our finding that myosin II is concentrated at the site of prehair formation, it seems plausible that it is actively involved in either the recruitment of F-actin to the prehair site, or that it directly participates in the assembly of actin bundles, or both. Studies of mammalian myosin II provide a precedent for a role in the formation of F-actin bundles. Phosphorylation of MRLC promotes a conformational change in myosin II from a folded to an extended state that readily forms multivalent bipolar filaments capable of binding multiple actin filaments (Tan et al., 1992). This is thought to result in F-actin bundling and stress fiber formation (Chrzanowska-Wodnicka and Burridge, 1996).

It appears that in the developing wing, the level of MRLC phosphorylation/myosin II activity must be within an optimal range to establish the formation of a single hair. It is possible that the efficiency of F-actin bundle formation is regulated by MRLC phosphorylation in a manner similar to the control of stress fiber formation. If one further assumes that there are certain bundling substrates present only at limiting concentrations (e.g., F-actin itself), then one would predict that the assembly of one F-actin bundle would reduce the probability of forming a second bundle. When MRLC phosphorylation falls below some threshold level (e.g., in *Drok* mutant cells), the efficiency of primary bundle formation is reduced, and thus the concentration of the limiting substrate remains at sufficient levels to support the assembly of secondary bundles/prehairs. Conversely, if MRLC is hyperphosphorylated (e.g., in Fz-overexpressing cells), the bundling efficiency may increase such that the threshold concentration for bundle formation would be reduced, thereby increasing the probability of assembling multiple bundles/prehairs. Future studies will be required to determine the detailed mechanisms involved.

Interaction of Myosin VIIA with the Fz/Dsh Pathway and Implications for Stereocilia Development

In addition to nonmuscle myosin II, which resembles the myosin II from skeletal muscle, there exists a large class of unconventional myosins that have different properties and potential functions in nonmuscle cells (reviewed in Mermall et al., 1998). For instance, several different classes of unconventional myosins are expressed in inner ear epithelium with different subcellular localization (Hasson et al., 1997). Mutations in three of the unconventional myosins, myosin VI, VIIA, and XV, cause hearing/balancing defects in mice, two of which when mutated in humans result in deafness (reviewed in Friedman et al., 1999). Of particular interest in the context of our study is myosin VIIA, mutations in which are responsible for mouse *shaker-1* and human Usher's syndrome 1B (Gibson et al., 1995; Weil et al., 1995). Loss-of-function *ck* (*Drosophila* Myosin VIIA) mutants exhibit a multiple hair and split wing hair phenotype (Figure 5E; Gubb et al., 1984; Turner and Adler, 1998). We have shown that *ck* exhibits strong genetic interactions with components of the signal transduction pathway defined in this study, and has opposite effects to that of myosin II. The seemingly antagonistic relationship between myosin II and myosinVIIA may suggest a mechanism in which the balance of the activities or stoichiometry of these two myosins is critical for the common process they regulate. For example, myosin II and myosin VIIA may share some common, limiting component(s) required for their activity. Thus, by reducing the myosin VIIA dose, myosin II has a larger share of the common component(s) and thus its activity is upregulated.

Recent evidence suggests that vertebrate homologs of Dsh and Fz regulate cell morphogenesis using pathways analogous to that of the *Drosophila* PCP pathway (reviewed in Sokol, 2000). Our findings raise the possibility that the Fz/Dsh cytoskeletal pathway (Figure 7) may also be at work in regulating cell polarity in vertebrates, including the stereocilia formation in the inner ear.

Experimental Procedures

Cloning and Mutant Mapping

Based on sequence similarity between the kinase domains of *Drosophila* Gek and mammalian Rho-kinase, degenerate RT-PCR was used to clone a fragment of *Drok* leading to the isolation of *Drok* cDNAs. Two overlapping cDNAs were sequenced on both strands, the composite of which constitutes an apparent full-length cDNA of 6.2 kb that agrees with the cDNA sequence reported by Mizuno et al. (GenBank accession number AF151375). The molecular nature of the *Drok*^{2} mutation was identified by comparing genomic sequence of heterozygous *Drok*^{2} and parental strains generated by PCR. To identify the consequence of *Drok*^{2} mutation, RT-PCR was performed on mRNA from hemizygous mutant and control larvae. Fragments that span from 39 base pairs before the end of exon 1 to 75 base pairs 3′ of the point mutation at the splice acceptor site were amplified and no difference was found in the level or apparent size of products. Sequencing of these PCR fragments revealed a single nucleotide deletion in *Drok*^{2} mutant.

Transgenic Constructs

tubP-Drok: Full-length *Drok* cDNA was cloned (KpnI-KpnI) into a modified pCaSpeR4 vector carrying the tubulin 1α promoter and a SV40 polyA signal sequence (Lee and Luo, 1999).

UAS-Drok-CAT and *UAS-Drok-CAT-KG*: The catalytic domain of Drok (aa 1–454) was cloned in pUAST (Brand and Perrimon, 1993). To create a kinase-dead version (UAS-Drok-CAT-KG), the conserved lysine (K116) required for ATP binding was changed to glycine by site-specific mutagenesis.

sqh transgenes: The sqhE21, A21, and A20A21 lines were previously described (Jordan and Karess, 1997), and the sqhE20E21 and E20A21 variants were constructed in a similar manner.

Generation of *Drok* Mutants

Drok was mapped by hybridization to a filter array of P1 clones (Genome Systems) to be within DSO1670, covered by a duplication *Tp(1;2)r*$^{+}$*75c*. To isolate *Drok* mutants, *y,w,FRT*^{19A} */Y;Pin/CyO, P[w*$^{+}$*]* flies were treated with 25 mM EMS (Ashburner, 1989), crossed with *C(1)DX/Y; Tp(1;2)r*$^{+}$*75c/SM1*. Single male *y,w, FRT*^{19A}*/Y; Tp(1;2)r*$^{+}$*75c/CyO, P[w*$^{+}$*]* progeny were mated with *XX/Y; her/SM1* females to determine if a lethal mutation covered by the duplication was present. Over 1500 such crosses were scored, with 22 lines showing *Tp(1;2)r*$^{+}$*75c* dependence. Two of these lines, *Drok*^{1} and *Drok*^{2}, were complemented by a *tubP-Drok* transgene.

Biochemistry

The GST pull-down assay between Drok and activated variants of purified GST-GTPases was performed as described in Luo et al. (1997). The binding buffer contained 0.05% Triton-X100. GST-RhoAV14 and GST-RhoAV14A37 were created by subcloning RhoAV14 cDNA into pGEX-4T1 between the BamHI and EcoRI sites. The GST-RhoAV14A37 variant was generated by oligo-directed mutagenesis.

Immunoblots (Figures 4A–4C): Extracts of 1st (A) or 3rd instar larvae (B and C) were prepared as per Young et al., 1993, but with the addition of 25 mM NaF, 20 mM $Na_4P_2O_7$, and 1 mM Na_3VO_4 to the extraction buffer. (B) The treated sample was prepared without phosphatase inhibitors and treated with 400 U λ phosphatase (New England Biolabs) for 30 minutes at 30°C. Expression of *UAS-Drok-CAT* and *UAS-Drok-CAT-KG* was induced by heat shock–regulated *Gal4* for 45 min at 38°C, followed by a 2 hr incubation at 25°C prior to extraction. Protein concentrations were determined (Bio-Rad Protein Assay). Thirty two μg of total protein/sample was separated by SDS-PAGE (14% acrylamide), blotted to a PVDF membrane (Immobilon-P; Millipore), and probed with affinity-purified rabbit anti-phospho-MRLC (Matsumura et al., 1998) diluted 1:200, or an anti-Sqh antibody (Jordan and Karess, 1997) at 1:200. Detection was performed with a donkey anti-rabbit $F(ab)^2$ fragment conjugated to HRP (Amerham) at 1:20,000 and ECL reagent (Amersham).

Mosaic Analysis of *Drok*^{2} Clones and Histology

FLP/FRT-mediated recombination was used to generate clones homozygous for *Drok*^{2} in the wing and eye imaginal discs, via heat shock–induced recombination in 1st instar larvae. Homozygous wing clones in pupae and newly eclosed adults were visualized using the MARCM system (Lee and Luo, 1999) by the presence of the membrane marker mCD8GFP. Genotypes: *y,w,Drok*^{2}*,FRT*^{19A}*/tubP-GAL80, hs-FLP, FRT*^{19A}*; UAS-mCD8GFP/+; tubP-Gal4/+* for pupal and early adult wing clones; *y,w,Drok*^{2}*,FRT*^{19A}*/tubP-GAL80, hs-FLP, FRT*^{19A} for adult eye clones.

At 32 hr, APF wings were dissected and fixed in 4% formaldehyde in PBT (100 mM phosphate buffer [pH 7.2] + 0.1% Tween-20). F-actin was stained with 200 nM Phalloidin-Alexa^{568nm} in PBT. Rabbit anti-myosin heavy chain (Zipper) (Jordan and Karess, 1997) or anti-phospho-MRLC antibody was used at 1:1000 or 1:20 in PBT, respectively. Secondary antibody was goat anti-rabbit-FITC (Jackson Labs, 1:200). Images were collected on a Bio-Rad MRC 1024 laser scanning confocal microscope and processed with NIH-Image1.62 and Adobe Photoshop 5.0.

Genetic Interaction Assays

dsh^1 interactions: Multiple hair phenotype was quantified in a rectangular area in the ventral marginal "cell", delimited on the proximal end by an orthogonal extending from the notch formed by the costal cell to wing vein II (wvII) and distally by the 15th stout marginal bristle (from the proximal end) to wvII. The number of multiple hair cells was counted and averaged for at least 10 wings per genotype.

hs-Fz interactions: The multiple hair phenotype was induced by heat shock at either 24 (early) or 30 hours (late) APF, in animals carrying one copy of *hs-Fz* (Krasnow and Adler, 1994). Quantification of the late phenotype was the same as for the *dsh*^{1} assay except that the proximal limit of the area scored was an orthogonal extending from the most proximal stout marginal bristle to wvII.

ck^{07130}*/sqh* interaction: The average number of multiple hair cells were counted within the ventral marginal "cell", from the notch formed by the costal cell to the distal end of the wing.

Acknowledgments

We thank M. Mlodzik for providing us with *RhoA* constructs, the Bloomington Stock Center for fly stocks, J. Reuter for technical assistance, and F. Matsumura for his generous gift of purified anti-phospho-MRLC. We thank M. Simon, C.-H. Yang, D. Kiehart, M. Cyert, and members of the Luo lab for their valued discussion during the course of the work. C. W. was supported by a National Institutes of Health postdoctoral fellowship. This work was supported by grants from the National Institutes of Health (R01 NS36623) and the Muscular Dystrophy Association to L. L., from the Cancer Research Fund of the Damon Runyon-Walter Winchell Foundation, Award DRS-16 to J. D. A., and from le Ministère de l'Éducation Nationale de la Recherche et de la Technologie and the Centre National de la Recherche Scientifique (France) (to A. R. and R. K.). L. L. was a Klingenstein, McKnight, and Sloan fellow or scholar.

Received September 22, 2000; revised February 9, 2001.

References

Amano, M., Ito, M., Kimura, K., Fukata, Y., Chihara, K., Nakano, T., Matsuura, Y., and Kaibuchi, K. (1996). Phosphorylation and activation of myosin by Rho-associated kinase (Rho-kinase). J. Biol. Chem. *271*, 20246–20249.

Amano, M., Chihara, K., Kimura, K., Fukata, Y., Nakamura, N., Matsuura, Y., and Kaibuchi, K. (1997). Formation of actin stress fibers and focal adhesions enhanced by Rho-kinase. Science *275*, 1308–1311.

Amano, M., Fukata, Y., and Kaibuchi, K. (2000). Regulation and functions of rho-associated kinase. Exp. Cell Res. *261*, 44–51.

Ashburner, M. (1989). Drosophila, A Laboratory Handbook (Cold Spring Harbor, NY: Cold Spring Harbor Press).

Ashburner, M., Misra, S., Roote, J., Lewis, S.E., Blazej, R., Davis, T., Doyle, C., Galle, R., George, R., Harris, N., et al. (1999). An exploration of the sequence of a 2.9-Mb region of the genome of *Drosophila melanogaster*. The Adh region. Genetics *153*, 179–219.

Axelrod, J.D., Miller, J.R., Shulman, J.M., Moon, R.T., and Perrimon, N. (1998). Differential recruitment of Dishevelled provides signaling specificity in the planar cell polarity and Wingless signaling pathways. Genes Dev. *12*, 2610–2622.

Boutros, M., Paricio, N., Strutt, D.I., and Mlodzik, M. (1998). Dishevelled activates JNK and discriminates between JNK pathways in planar polarity and wingless signaling. Cell *94*, 109–118.

Brand, A.H., and Perrimon, N. (1993). Targeted gene expression as a means of altering cell fates and generating dominant phenotypes. Development *118*, 401–415.

Chen, T.L., Edwards, K.A., Lin, R.C., Coats, L.W., and Kiehart, D.P. (1991). *Drosophila* myosin heavy chain at 35BC. J. Cell Biol. *115*, 330a.

Chrzanowska-Wodnicka, M., and Burridge, K. (1996). Rho-stimulated contractility drives the formation of stress fibers and focal adhesions. J. Cell Biol. *133*, 1403–1415.

Eaton, S. (1997). Planar polarization of *Drosophila* and vertebrate epithelia. Curr. Opin. Cell Biol. *9*, 860–866.

Eaton, S., Wepf, R., and Simons, K. (1996). Roles for Rac1 and Cdc42 in planar polarization and hair outgrowth in the wing of *Drosophila*. J. Cell Biol. *135*, 1277–1289.

Fanto, M., Weber, U., Strutt, D.I., and Mlodzik, M. (2000). Nuclear signaling by Rac and Rho GTPases is required in the establishment of epithelial planar polarity in the *Drosophila* eye. Current Biol. *10*, 979–988.

Friedman, T.B., Sellers, J.R., and Avraham, K.B. (1999). Unconventional myosins and the genetics of hearing loss. Amer. J Med. Genet. *89*, 147–157.

Gibson, F., Walsh, J., Mburu, P., Varela, A., Brown, K.A., Antonio, M., Beisel, K.W., Steel, K.P., and Brown, S.D.M. (1995). A type VII myosin encoded by the mouse deafness gene shaker-1. Nature *374*, 62–64.

Gubb, D., and Garcia-Bellido, A. (1982). A genetic analysis of the determination of cuticular polarity during development in *Drosophila melanogaster*. J. Embryol. Exp. Morph. *68*, 37–57.

Gubb, D., Shelton, M., Roote, J., McGill, S., and Ashburner, M. (1984). The genetic analysis of a large transposing element of *Drosophila melanogaster*. The insertion of a w+ rst+ TE into the ck locus. Chromosoma *91*, 54–64.

Hall, A. (1998). Rho GTPases and the actin cytoskeleton. Science *279*, 509–514.

Hasson, T., Gillespie, P. G., Garcia, J. A., MacDonald, R. B., Zhao, Y.-d., Yee, A. G., Mooseker, M. S., and Corey, D. P. (1997). Uncon-

ventional myosins in inner-ear sensory epithelia. J. Cell Biol. *137*, 1287–1307.

Ishizaki, T., Maekawa, M., Fujisawa, K., Okawa, K., Iwamatsu, A., Fujita, A., Watnabe, N., Saito, Y., Kakizuka, A., Morii, N., and Narumiya, S. (1996). The small GTP-binding protein Rho binds to and activates a 160 kDa Ser/Thr protein kinase homologous to myotonic dystrophy kinase. EMBO J. *15*, 1885–1893.

Ishizaki, T., Naito, M., Fujisawa, K., Maekawa, M., Watanabe, N., Saito, Y., and Narumiya, S. (1997). p160ROCK, a Rho-asociated coiled-coil forming protein kinase, works downstream of Rho and induces focal adhesions. FEBS Lett. *404*, 118–124.

Jordan, P., and Karess, R. (1997). Myosin light chain-activating phosphorylation sites are required for oogenesis in *Drosophila*. J. Cell Biol. *139*, 1805–1819.

Karess, R.E., Chang, X.J., Edwards, K.A., Kulkarni, S., Aguilera, I., and Kiehart, D.P. (1991). The regulatory light chain of nonmuscle myosin is encoded by spaghetti-squash, a gene required for cytokinesis in *Drosophila*. Cell *65*, 1177–1189.

Kimura, K., Ito, M., Amano, M., Chihara, K., Fukata, Y., Nakafuku, M., Yamamori, B., Feng, J., Nakano, T., Okawa, K., et al. (1996). Regulation of myosin phosphatase by Rho and Rho-associated kinase (Rho-kinase). Science *273*, 245–248.

Klingensmith, J., Nusse, R., and Perrimon, N. (1994). The *Drosophila* segment polarity gene dishevelled encodes a novel protein required for response to the wingless signal. Genes Dev. *8*, 118–130.

Krasnow, R.E., and Adler, P.N. (1994). A single frizzled protein has a dual function in tissue polarity. Development *120*, 1883–1893.

Krasnow, R.E., Wong, L.L., and Adler, P.N. (1995). Dishevelled is a component of the frizzled signaling pathway in *Drosophila*. Development *121*, 4095–4102.

Lee, T., and Luo, L. (1999). Mosaic analysis with a repressible cell marker for studies of gene function in neuronal morphogenesis. Neuron *22*, 451–461.

Leung, T., Chen, X.-Q., Manser, E., and Lim, L. (1996). The p160 Rho-binding kinase ROKa is a member of a kinase family and is involved in the reorganization of the cytoskeleton. Mol. Cell Biol. *16*, 5313–5327.

Luo, L., Lee, T., Tsai, L., Tang, G., Jan, L.Y., and Jan, Y.N. (1997). Genghis Khan (Gek) as a putative effector for *Drosophila* Cdc42 and regulator of actin polymerization. Proc. Natl. Acad. Sci. USA *94*, 12963–12968.

Matsumura, F., Ono, S., Yamakita, Y., Totsukawa, G., and Yamashito, S. (1998). Specific localization of serine 19 phosphorylated myosin II during cell locomotion and mitosis of cultured cells. J. Cell Biol. *140*, 119–129.

Matsui, T., Amano, M., Yamamoto, T., Chihara, K., Nakafuku, M., Ito, M., Nakano, T., Okawa, K., Ewamatsu, A., and Kaibuchi, K. (1996). Rho-associated kinase, a novel serine/threonine kinase, as a putative target for the small GTP binding protein Rho. EMBO J. *15*, 2208–2216.

Mermall, V., Post, P.L., and Mooseker, M.S. (1998). Unconventional myosins in cell movement, membrane traffic, and signal transduction. Science *279*, 527–532.

Mizuno, T., Amano, M., Kaibuchi, K., and Nishida, Y. (1999). Identification and characterization of *Drosophila* homolog of Rho-kinase. Gene *238*, 437–444.

Mlodzik, M. (1999). Planar polarity in the *Drosophila* eye: a multifaceted view of signaling specificity and cross-talk. EMBO J. *18*, 6873–6879.

Self, T., Mahony, M., Fleming, J., Walsh, J., Brown, S.D.M., and Steel, K.P. (1998). Shaker-1 mutations reveal roles for myosin VIIA in both development and function of cochlear hair cells. Development *125*, 557–566.

Shulman, J.M., Perrimon, N., and Axelrod, J.D. (1998). Frizzled signaling and the developmental control of cell polarity. Trends Genet. *14*, 452–458.

Sokol, S. (2000). A role for Wnts in morphogenesis and tissue polarity. Nature Cell Biol. *2*, E1–E2.

Spradling, A.C., Stern, D., Beaton, A., Rhem, E.J., Laverty, T., Mozden, N., Misra, S., and Rubin, G.M. (1999). The Berkeley *Drosophila* genome project gene disruption project. Single P-element insertions mutating 25% of vital *Drosophila* genes. Genetics *153*, 135–177.

Strutt, D.I., Weber, U., and Mlodzik, M. (1997). The role of RhoA is tissue polarity and Frizzled signaling. Nature *387*, 292–295.

Tan, J.L., Ravid, S., and Spudich, J.A. (1992). Control of nonmuscle myosins by phosphorylation. Annu. Rev. Biochem. *61*, 721–759.

Theisen, H., Purcell, J., Bennett, M., Kansagara, D., Syed, A., and Marsh, J.L. (1994). dishevelled is required during wingless signaling to establish both cell polarity and cell identity. Development *120*, 347–360.

Tilney, L.G., and Tilney, M.S. (1992). Actin, filaments, sterocilia and hair cells: how cells count and measure. Annu. Rev. Cell Biol. *8*, 257–274.

Turner, C.M., and Adler, P.N. (1998). Distinct roles for the actin and microtubule cytoskeletons in the morphogenesis of epidermal hairs during wing development in *Drosophila*. Mech. Dev. *70*, 181–192.

Usui, T., Shima, Y., Shimada, Y., Hirano, S., Burgess, R.W., Schwarz, T.L., Takeichi, M., and Uemura, T. (1999). Flamingo, a seven-pass transmembrane cadherin, regulates planar cell polarity under the control of Frizzled. Cell *98*, 585–595.

Vinson, C.R., Conover, S., and Adler, P.N. (1989). A *Drosophila* tissue polarity locus encodes a protein containing seven potential transmembrane domains. Nature *338*, 263–264.

Weber, U., Paricio, N., and Mlodzik, M. (2000). Jun mediates frizzled-induced R3/R4 cell fate distinction and planar polarity determination in the *Drosophila* eye. Development *127*, 3619–3629.

Weil, D., Blanchard, S., Kaplan, J., Guilford, P., Gibson, F., Walsh, J., Mburu, P., and Varela, A. (1995). Defective myosin VIIA gene responsible for Usher syndrome type 1B. Nature *374*, 62–65.

Wissmann, A., Ingles, J., McGhee, J.D., and Mains, P.E. (1997). Caenorhabditis elegans LET-502 is related to Rho-binding kinases and human myotonic dystrophy kinase and interacts genetically with a homolog of the regulatory subunit of smooth muscle myosin phosphatase to affect cell shape. Genes Dev. *11*, 409–422.

Wodarz, A., and Nusse, R. (1998). Mechanisms of Wnt signaling in development. Annu. Rev. Cell Dev. Biol. *14*, 59–88.

Wong, L.L., and Adler, P.N. (1993). Tissue polarity genes of *Drosophila* regulate the subcellular location for prehair initiation in pupal wing cells. J. Cell Biol. *123*, 209–221.

Young, P.E., Richman, A.M., Ketchum, A.S., and Kiehart, D.P. (1993). Morphogenesis in *Drosophila* requires nonmuscle myosin heavy chain function. Genes Dev. *7*, 29–41.

Zheng, L., Zhang, J., and Carthew, R.W. (1995). Frizzled regulates mirror-symmetric pattern formation in the *Drosophila* eye. Development *121*, 3045–3055.